Local periodic poling of ridges and ridge waveguides on X- and Y-Cut LiNbO₃ and its application for second harmonic generation

L. Gui*, H. Hu, M. Garcia-Granda, and W. Sohler

Angewandte Physik, Universität Paderborn, 33098 Paderborn, Germany
[*]Corresponding author: lgui@mail.upb.de

Abstract: Fabrication, characterization and application of periodical ferroelectric domains in ridges and Ti in-diffused ridge waveguides on X- and Y-cut Lithium Niobate (LN) are reported. The ridge waveguides of 3.5 µm height and 9 µm width were fabricated by inductively coupled plasma (ICP) etching followed by Ti in-diffusion into the ridges only. Appropriate electrodes on their side walls enabled domain inversion restricted to the ridge. The domain structure was investigated by selective chemical etching. Second harmonic generation in a 1.4 cm long ridge waveguide on an X-cut substrate was demonstrated at 1548 nm fundamental wavelength with an efficiency of 17% W^{-1}.

OCIS codes: (160.3730) Lithium niobate; (160.2260) Ferroelectrics; (230.7370) Waveguides; (190.2620) Harmonic generation.

References and links

1. M. A. Foster, A. C. Turner, M. Lipson, and A. L. Gaeta, "Nonlinear optics in photonic nanowires," Opt. Express **16**, 1300-1320 (2008).
2. H. Hu, R. Ricken, W. Sohler, and R. B. Wehrspohn: "Lithium niobate ridge waveguides fabricated by wet etching," IEEE Photon. Technol. Lett. **19**, 417-419 (2007).
3. K.Mizuuchi, K. Yamamoto, and M. Kato, "Harmonic blue light generation in X-cut MgO:LiNbO₃ waveguide," Electron. Lett. **33**, 806-807 (1997).
4. T. Sugita, K. Mizuuchi. Y. Kitaoka, and K. Yamamoto, "Ultraviolet light generation in a periodically poled MgO:LiNbO₃ waveguide," Jpn. J. Appl. Phys. **40**, 1751-1753 (2001).
5. T. Kishino, R. F. Tavlykaev, and R. V. Ramaswamy, "70+ µm deep domain inversion in X-cut LiNbO₃ and its use in a high-speed bandpass integrated-optic modulator," Appl. Phys. Lett. **76**, 3852-3854 (2000).
6. S. Sonoda, I. Tsuruma, and M. Hatori, "Second harmonic generation in a domain-inverted MgO-doped LiNbO₃ waveguide by using a polarization axis inclined substrate," Appl. Phys. Lett. **71**, 3048-3050 (1997).
7. S. Sonoda, I. Tsuruma, and M. Hatori, "Second harmonic generation in electric poled X-cut MgO-doped LiNbO₃ waveguides," Appl. Phys. Lett. **70**, 3078-3080 (1997).
8. K. Mizuuchi, T. Sugita, K. Yamamoto, T. Kawaguchi, T. Yoshino, and M. Imaeda, "Efficient 340-nm light generation by a ridge-type waveguide in a first-order periodically poled MgO:LiNbO₃," Opt. Lett. **28**, 1344-1346 (2003).
9. Y. Nishida, H. Miyazawa, M. Asobe, O. Tadanaga, and H. Suzuki, "0-dB wavelength conversion using direct-bonded QPM-Zn:LiNbO₃ ridge waveguide," IEEE Photon. Technol. Lett. **17**, 1049-1051 (2005).
10. F. Généreux, G. Baldenberger, B. Bourliaguet, and R. Vallée: "Deep periodic domain inversion in X-cut LiNbO₃ and its use for second harmonic generation near 1.5 µm," Appl. Phys. Lett. **91**, 231112 (2007).
11. H. Hui, Applied Physics, University of Paderborn, 33098 Paderborn, Germany, is preparing a manuscript to be called "Self-aligned metal-deposition on ridge structures for diffusion doping and electrode definition".
12. M. Garcia-Granda, "High bandwidth integrated optical ridge guide modulators," European Ph.D. thesis (submitted to the University of Oviedo and to the University of Paderborn in Dec. 2008).
13. D. Hofmann, "Nichtlineare, integriert optische Frequenzkonverter für das mittlere Infrarot mit periodisch gepolten Ti:LiNbO₃ –Streifenwellenleitern," 147-165, Ph.D.-thesis, University of Paderborn, 2001.
14. G. Rosenman, V. D. Kugel, and D. Shur, "Diffusion-induced domain inversion in ferroelectrics," Ferroelectrics **172**, 7-18 (1995).
15. G. Berth, V. Wiedemeier, K-P. Hüsch, L. Gui, H. Hu, W. Sohler, and A. Zrenner, "Imaging of ferroelectric micro-domains in X-cut lithium niobate by confocal second harmonic microscopy," Ferroelectrics, in press.
16. R. Regener and W. Sohler, "Loss in low-finesse Ti:LiNbO₃ optical waveguide resonators," Appl. Phys. B **36**, 143-147 (1985).

1. Introduction

To enhance the efficiency of nonlinear interactions in optical waveguides, smaller cross section and higher index contrast are required leading to a stronger enhancement of the guided mode intensity. Therefore, "photonic nanowires" are currently developed [1]. If ferroelectric materials like Lithium Niobate (LN) are considered, a periodic domain inversion is required to enable quasi phase matching (QPM) for second order nonlinear processes. Ridge waveguides represent a first step towards photonic nanowires; they can be fabricated with excellent properties on Z-cut LN by chemical etching [2]. Besides Z-cut LN, also X-cut and Y-cut LN with periodically poled domain structure are of increasing interest. Several approaches for periodic domain inversion on planar surfaces of X- and Y-cut LN have been proposed [3-7]. On the other hand, periodically poled ridge guides were fabricated by lapping, polishing and mechanical micro-machining periodically poled LN (PPLN) layers, glued or bonded, respectively, to a LN substrate [8,9]. Recently, also a deep domain inversion in an 84 µm wide ridge on X-cut LN with a proton exchanged channel guide in its centre was reported [10].

In contrast to all mentioned approaches, we report in this contribution local periodic poling of ridges and Ti in-diffused ridge waveguides on X- and Y-cut LN fabricated by inductively coupled plasma (ICP) etching. Local poling was enabled by appropriate electrodes defined on the side walls of the ridges. The resulting domain structures were investigated in all three dimensions by preferential chemical etching and optical microscopy. Second harmonic generation in a periodically poled ridge guide with localized domain structure on X-cut LN is demonstrated.

2. Sample fabrication

Waveguide fabrication, electrode definition, and poling procedure are nearly identical for X-cut and Y-cut LN; therefore, we describe these processes using X-cut LN as an example.

2.1 Waveguide fabrication

A Cr film of 220 nm thickness was deposited by sputtering on the –X face of an X-cut LN substrate of 1 mm thickness. Using optical contact lithography with an e-beam written mask and wet etching with a Cerium Sulfate solution, Cr stripes of typically 9 µm width were defined. The Cr stripes served as etch mask for the successive ICP (inductively coupled plasma) etching of LN with an etching ratio of 1:10 (Cr:LN). The etching gas was a mixture of 15 sccm C_4F_8 and 15 sccm He. After 4 minutes, the sample was taken out and cleaned in SC-1 (RCA) solution (70% H_2O, 20% H_2O_2, 10% NH_4OH) for 1 minute to remove a brown layer, probably carbon polymers; then the etching was continued. This process was repeated 10 times until the etching depth was ~3 µm. Finally, the remaining Cr stripe was removed by a Cerium Sulfate solution and the sample was carefully cleaned. Optical guiding in the vertical direction was obtained by in-diffusing a 70 nm thick Ti-stripe into the ridge. The key technique of depositing Ti just on top of ridge will be explained in another contribution [11]. Ti in-diffusion has been done at ~1060°C for 8.5 hours. Fig. 1 shows SEM micrographs of etched ridges on X-cut LN of ~3.5 µm height before and after Ti in-diffusion, respectively. Before the in-diffusion the surface of the LN substrate was very rough due to the ICP etching process; it was considerably smoothed during annealing at the high diffusion temperature.
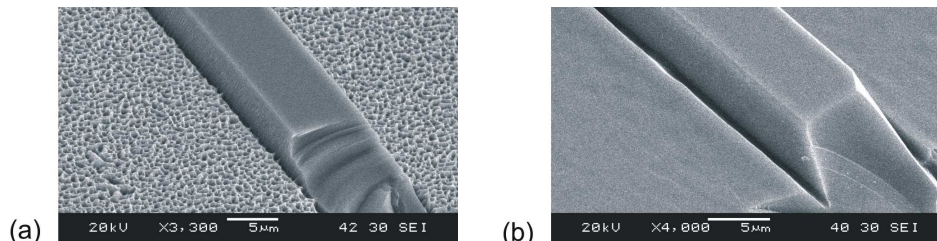

Fig. 1. SEM micrographs of (a) an etched ridge and (b) a Ti in-diffused ridge waveguide on X-cut LN.

2.2 Electrodes definition and electric field assisted poling

A scheme of the ridge waveguide with a comb like electrode structure on both sides of the ridge is depicted in Fig. 2. According to the simulation of the electric field distribution (Fig. 3), such a configuration is ideal to get microdomain inversion only in the body of the ridge with a relatively low poling voltage. The static electric potential distribution was calculated in the cross section of the ridge using a finite difference method; homogeneous electrodes have been assumed for the calculations. A numeric derivation was made on a non-uniform grid of 512x512 points in an area of 60x50 μm^2 around the ridge, yielding as result the profile of the relevant component (E_z) of the electric field distribution [12]. Fig. 3 presents as example lines of constant E_z in a ridge of 4.0 µm height and 9 µm width at the top, assuming 1 V applied to the left electrode and the right electrode grounded. As the coercive field of LN is ~20 MV/m, the applied voltage should be at least 166 V to start domain inversion. First nucleation is expected at the upper edge of the ridge where the field is highest. In most of the cases, due to the imperfection of the electrodes, the actual applied voltage had to be higher than the simulated value.

To fabricate comb like electrodes, we used lift-off lithography of a vacuum-deposited, 70 nm thick Ti layer. A micrograph of a fabricated electrode structure is shown as inset of Fig. 2. The poling experiments were done in an oil bath to maintain a high resistance between the two electrodes and to avoid surface currents as much as possible. Up to 5 high voltage pulses with different pulse durations were applied for poling. We observed that the largest charge is accumulated during the first pulse; it decreases fast with increasing pulse number indicating that most of the domain inversion has been achieved by the first pulse alone. Such a behavior has already been observed previously [13]. Therefore, in more recent experiments, we used only one or two pulses to achieve domain inversion. Moreover, we observed considerable differences for poling undoped and Ti-doped ridges.
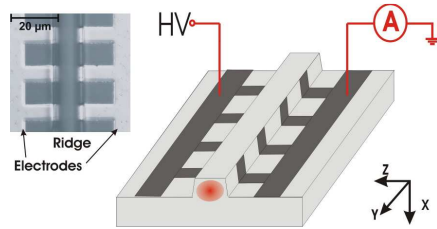

Fig. 2. Scheme of the poling configuration for a ridge on X-cut LN. Inset: Top view of the electrodes of 16.6 µm period for a 9 µm wide ridge.

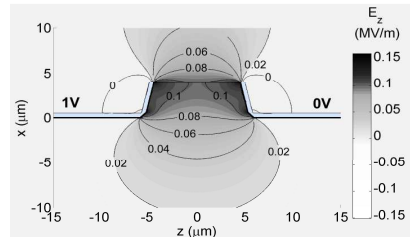Fig. 3. Calculated E_z (MV/m) in a ridge of 4 µm height and 9 µm width, assuming 1 V applied to the left electrode with the right electrode grounded.

Figure 4(a) presents a typical current-time characteristic for poling an undoped ridge with a single voltage pulse. The voltage is ramped up with a slope of 80 V/ms, kept constant for 15 ms, then ramped down to zero with the same slope. In parallel, the poling current was monitored. The current abruptly rises when the voltage reaches ~180 V, indicating the start of domain inversion consistent with the theoretical value given above. A second rise of the current appears when the voltage ramps up to ~300V, indicating domain inversion in a larger area. However, the current decrease after reaching the constant voltage is hard to be explained. Afterwards, the current nearly stabilizes as long as the constant voltage is applied. Then it drops to zero as the voltage ramps down. Considering the spontaneous polarization of congruent LN of 0.72 µC/mm² at room temperature and the poled area of ~0.1 mm² (four ridges were poled simultaneously), the total charge required for poling should be 0.14 µC. This value is significantly smaller than the measured total charge of ~1 µC. We suspect that there might be some leakage current along the surface involved.

In the case of poling a Ti in-diffused ridge waveguide, domain inversion starts at a considerably higher voltage of ~350V (see Fig. 4(b)); this could be due to Li out-diffusion during

annealing at the high diffusion temperature resulting in the formation of a thin domain inverted layer on one side of the ridge (see also [14]). We had to use a longer pulse of higher voltage to achieve domain inversion.
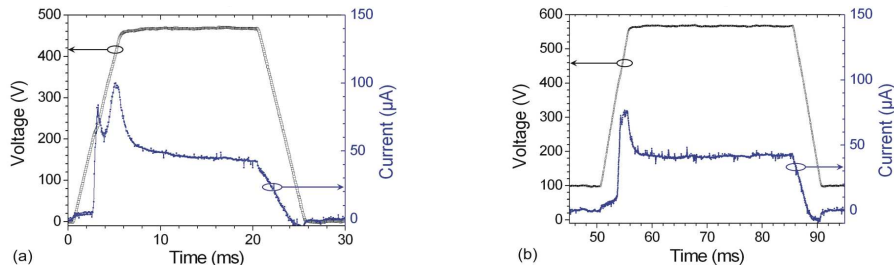

Fig. 4. Poling voltage and resulting poling current as a function of time for single pulse poling of (a) a ridge and (b) a Ti in-diffused ridge waveguide on X-cut LN.

3. Characterization of Microdomains

To reveal the shape and uniformity of the ferroelectric microdomains, the samples were first immersed in HF:HNO$_3$ for 30 minutes, and then observed from the top using (differential interference contrast) optical microscopy. Figures 5(a) and 6(a) present corresponding results of the upper surface of selectively etched undoped ridges on X- and Y-cut substrates, respectively. In Fig. 5(a) a periodical etching of the side walls is observed, whereas in Fig. 6(a) in addition a periodical modulation of the height of the ridge can be seen. In the inverted domains both directions of Z- and Y-axis are rotated by 180º; the crystallographic X-axis will remain the same. Therefore, the side walls consist of a sequence of +Z- and –Z-faces, whereas the top surface is either a homogeneous X-face (Fig. 5(a)) or a periodical sequence of +Y- and –Y-faces (Fig. 6(a)). This explains the observed patterns after etching, as +Z and –Z faces of LN, as well as +Y and –Y faces, have significantly different etching rates in HF: HNO$_3$.

Afterwards the samples have been cut through the body of the ridge as shown in Figs. 5(d) and 6(d) and etched in HF:HNO$_3$ for another 10 minutes. In this way the +Z- and –Z-faces of the periodical domain structure can be observed on the sidewall and in the body of the ridges. Due to the different etching rates the inverted domains become visible (Figs. 5(b)-5(c) and 6(b)-6(c)). In the ridge on the X-cut substrate a hexagonal shape is observed as marked with white dash lines in Fig. 5(c). The depth of the domains (in X-direction) corresponds to the height of the ridge as expected. The duty cycle of the periodical domain structure is ~7:3 (width of inverted to non-inverted domain). This means some over-poling in comparison with the duty cycle of the finger electrodes of 1:1. The ridge on the Y-cut substrate (Fig. 6) was poled with finger electrodes of a duty cycle of 4:6 (finger width: interval width) resulting in an improved duty cycle of the domain structure close to 1:1. However, the shape of the domains is significantly different with a depth somewhat smaller than on the X-cut substrate.
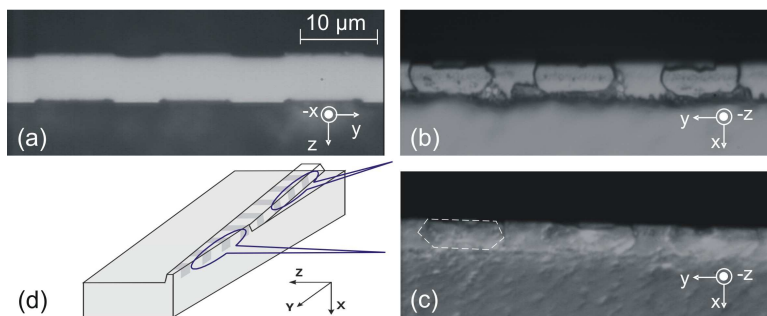

Fig. 5. Selectively etched, periodically poled ridge on X-cut LN. (a) Top view. (b) Side view. (c) Side view after cutting the ridge. (d) Cutting scheme.
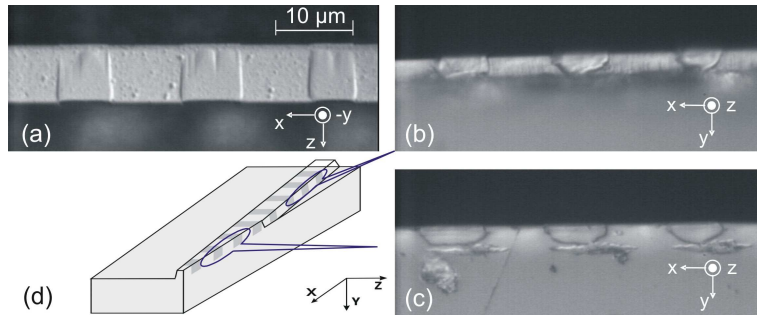
Fig. 6. Selectively etched, periodically poled ridge on Y-cut LN. (a) Top view. (b) Side view. (c) Side view after cutting the ridge. (d) Cutting scheme. In (c) also horizontal marks, resulting from a previous, not fully successful experiment can be seen below the domains.

A further investigation of periodically poled ridges using confocal second harmonic microscopy essentially confirmed the presented results and gave some additional information on the 3-dimensional structure of the domains [15].

4. Second harmonic generation

Second harmonic generation (SHG) was investigated using a periodically poled Ti in-diffused ridge waveguide on X-cut LN of 3.5 µm height and 9 µm width. The length and the period of the periodically poled section are 14 mm and 16.6 µm respectively. The end faces of the waveguide have been carefully polished; no anti-reflection coating was deposited. An external cavity laser was used to tune the fundamental wavelength λ_f in steps of 1 pm around λ_f = 1548 nm. The light was coupled to the waveguide by fiber butt coupling with some index matching oil between fiber and waveguide end face. In this way the reflectivity of the front face was reduced to about 3.6 %; the rear face still had a reflectivity of ~14 %, determined by the index step between LN and air. Figure 7 presents the SHG tuning characteristic as generated second harmonic power versus λ_f around 1548 nm together with the transmitted fundamental power. Fabry-Perot resonances are observed determined by the cavity with 3.6 % and 14 % mirror reflectivities. They allow evaluating precisely the propagation losses of here 1.0 dB/cm [16]. As this value is an upper limit for the actual losses, the good quality of the waveguide is demonstrated. The intra-cavity modulated fundamental power in turn modulates the generation of the second harmonic power. Due to the nonlinear interaction the corresponding resonances become narrower; moreover, they are also modified by Fabry-Perot resonances at the second harmonic wavelength λ_{SH} (see inset of Fig. 7). Fitting a theoretical SHG tuning characteristic to the average of the experimental result yields a good agreement of theoretical and measured bandwidth of 0.8 nm demonstrating the excellent homogeneity of the periodically poled waveguide along the interaction length.

SHG was also investigated as function of the fundamental power up to 140 mW; the result is shown in Fig. 8. At low power levels a parabolic dependence was observed, well described by a power normalized efficiency of 17 % W^{-1} (or 8.5 % $W^{-1} cm^{-2}$). It is calculated as the ratio of out-coupled SH-power and the square of in-coupled fundamental power. At higher fundamental power levels a weaker growth of the SH-power up to ~2 mW was measured. This indicates the onset of photorefractive effects deteriorating phase matching of the nonlinear interaction. The insets of Fig. 8 show the transmitted fundamental modes of TE-polarization for both fundamental wave (inset1) and generated second harmonic wave (inset2); a dotted line in inset1 sketches the shape of the ridge.
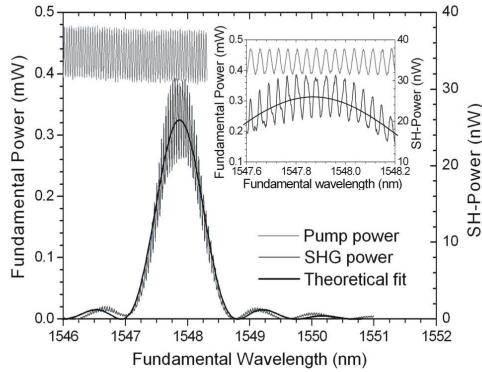
Fig. 7. Generated SH- and transmitted fundamental powers as a function of the fundamental wavelength for a 14 mm long, periodically poled ridge waveguide on X-cut LN. Inset: Results around the maximum efficiency plotted with higher resolution.
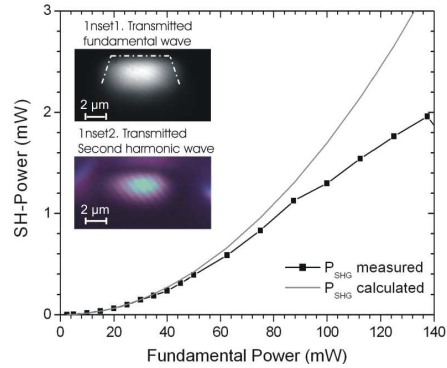
Fig. 8. Generated SH-power as a function of in-coupled fundamental power. Insets: Mode distributions at the output of the ridge guide.

The measured normalized efficiency of 8.5 % W^{-1} cm^{-2} is somewhat lower than the efficiency of about 11 % W^{-1} cm^{-2} of Ti:LN standard waveguides (diffused into a planar Z-cut surface). This is due to higher propagation losses, a non-ideal duty cycle of the domain structure, and ridge dimensions larger than necessary for maximum SHG. By reducing ridge dimensions, the size of the fundamental mode can become significantly smaller than the mode of a Ti:LN standard waveguide. This would improve the overlap of fundamental and second harmonic modes resulting in a considerable improvement of the nonlinear efficiency.

5. Conclusions

In conclusion, inductively coupled plasma- (ICP-) etching enabled fabricating ridges of micrometer cross section dimension of good quality on X- and Y-cut LN. To define optical waveguides, Ti was in-diffused in the ridge only. Due to the high diffusion temperature, the roughness of the ridge walls was significantly reduced lowering in this way the propagation losses. By depositing electrodes on the side walls of the ridge, a fabrication of (periodic) microdomains localized in the body of the ridge became possible; poling required relatively low voltages of a few hundred volts only. Selective chemical etching revealed shape and depth of the inverted domains. The depth of about 3.5 µm guarantees a good overlap with the guided optical modes at 1.5 µm wavelength. Second harmonic generation in a periodically poled ridge waveguide of 14 mm length was demonstrated with an efficiency of 17 % W^{-1}.

Further work is underway to improve the quality of the ridge waveguides, in particular, to reduce the propagation losses and to optimize the duty cycle of the periodic domains. Moreover, ridge waveguides of smaller cross section will be developed to get a stronger mode confinement and overlap. In this way a significant increase of the SHG-efficiency can be expected. Also materials of lower photorefractive susceptibility such as MgO:LN will be used to fabricate proton exchanged PPLN ridge guides with the same poling technique. As a consequence, higher SH power levels should become possible.

Acknowledgments